Rotational Spectra of $^{14}N^{17}O$ and $^{15}N^{18}O$

Axel H. Saleck[1], Martin Liedtke, Alexandra Dolgner, and Gisbert Winnewisser
I. Physikalisches Institut, Zülpicher Straße 77, D-50937 Köln

Z. Naturforsch. **49a,** 1111–1118 (1994); received September 16, 1994

The mm-wave spectra of $^{15}N^{18}O$ and $^{14}N^{17}O$ in both $X^2\Pi_{1/2}$ and $X^2\Pi_{3/2}$ states have been measured and assigned for the first time. Improved rotational and, for the first time, ^{17}O hyperfine coupling constants have been derived from the analysis. The $^{14}N^{17}O$ data yield parameters of the unpaired electron spatial distribution near both nuclei. Furthermore, the deviation from the Born-Oppenheimer approximation is confirmed on the basis of the rotational constants of five isotopomers. Finally, when comparing the nuclear spin-rotation constants to the ones of other molecules containing ^{14}N or ^{17}O nuclei, a roughly linear proportionality with the rotational constant B is found.

1. Introduction

Rotational spectra of diatomic molecules bear fundamental information on molecular structure and the chemical bond. The rotational energies are characterized by three contributions: First of all, the moment of inertia of the molecular frame determines the pure rotational contribution. Therefore, rotational spectroscopy yields the most precise determination of bond lengths. By careful analyses of rotational transitions of different isotopomers in several vibrational states, a slight dependence of the internuclear equilibrium distance on the isotopic constitution has been detected for several molecules and interpreted as a deviation from the Born-Oppenheimer approximation (e.g. [1–4]). Theoretical corrections to the Born-Oppenheimer approximation have been given by Watson [1, 5] and Bunker [6]. As to experimental contributions, an extensive study on observed adiabatic and non-adiabatic corrections to the Born-Oppenheimer approximation has been performed for more than 10 diatomic molecules by Tiemann et al. [2]. For such studies, it is desirable to have a maximum of rotational spectra of different isotopomers and vibrational states for a given molecule.

A second effect in rotational spectra will occur if the molecule is a radical. Then, the presence of electronic spin or electronic angular momentum leads to a fine structure. Finally, nonzero nuclear spins give rise to hyperfine structure (hfs). In both cases it is the spatial distribution of the unpaired electron(s) that determines the magnitude of the effects, and thus the related molecular parameters contain information on the electronic distribution. CN is an example where all three contributions appear. For this radical, recently laboratory and astronomical rotational spectra have been combined to derive the related molecular parameters [3].

One of the fundamental diatomic radicals is nitric oxide. Among NO isotopic species, rotational spectra of $^{14}N^{16}O$, $^{15}N^{16}O$, and $^{14}N^{18}O$ have been observed in their ground states by mm- and submm-wave high-resolution spectroscopy within recent years [4, 7]. In [4], these measurements were used to study the isotopic dependence of rotational constants; a slight breakdown of the Born-Oppenheimer approximation had been detected as judged by the reduced mass dependence of the rotational constant B.

Here we present high-resolution mm-wave measurements of $^{15}N^{18}O$ and $^{14}N^{17}O$ in both $X^2\Pi_{1/2}$ and $X^2\Pi_{3/2}$ states. In combination with the results from vibrational spectroscopy, performed by Teffo et al. [8] and Amiot et al. [9], the new data allow us to check the reduced mass dependence of B found in [4]. As one result, the mentioned deviation from the Born-Oppenheimer approximation can be confirmed now on the basis of rotational constants of five – instead of three – isotopomers.

The only oxygen nucleus with nonvanishing nuclear spin is ^{17}O. The ^{17}O hyperfine structure parameters, determined for the first time in nitric oxide, and their ^{14}N counterparts allow us to obtain parameters of the electronic orbital distribution near both nuclei in this diatomic molecule.

---

[1] Present address: Institute for Molecular Science, Myodaiji, Okazaki 444, Japan.

Reprint requests to Prof. G. Winnewisser.

0932-0784 / 94 / 1200-1111 $ 06.00 © – Verlag der Zeitschrift für Naturforschung, D-72027 Tübingen

Finally, the very small nuclear-spin rotation coupling constants for both nuclei will be compared to the ones for other linear molecules.

2. Experimental Procedure

The spectra of both isotopomers, $^{15}N^{18}O$ and $^{14}N^{17}O$, could not be recorded in natural abundance. The ^{18}O and ^{17}O enrichment was achieved by adding enriched water ($H_2{}^{18}O$: 37.0%, $H_2{}^{17}O$: 2.74%) to dinitrogen tetroxide N_2O_4 at a temperature of $-20\,^\circ C$, followed by the chemical reaction [10]

$$H_2O + N_2O_4 \rightarrow HNO_2 + NHO_3. \tag{1}$$

To free nitric oxide, mercury and sulphuric acid were added to the mixture of nitrous and nitric acid, as described in [4]. The final concentrations in the gaseous sample were estimated to lie at about 0.5% $^{14}N^{17}O$ and 0.03% $^{15}N^{18}O$.

For the observation of the $J = 3/2 \leftarrow 1/2$ lines, at 137 GHz ($^{15}N^{18}O$) and 146 GHz ($^{14}N^{17}O$), the spectrometer was used in the configuration previously described [11]; the $J = 5/2 \leftarrow 3/2$ transitions were measured using a phase-locked backward wave oscillator (Carcinotron, Thomson- CSF) as frequency source.

79 transitions of $^{14}N^{17}O$ and 13 of $^{15}N^{18}O$ were recorded in the frequency range between 137 and 251 GHz at pressures of 25–40 μbar. They are listed in Tables 1–3, together with estimates of their experimental uncertainties. Figure 1 shows a portion of the observed hyperfine pattern of the $^2\Pi_{1/2}$ $J = 5/2 \leftarrow 3/2$ transition of $^{14}N^{17}O$ at 244.0 GHz.

For better recognition of the $^{15}N^{18}O$ spectra at 137 GHz, observed with a frequency-doubled Gunn oscillator, reference spectra without sample were recorded and subtracted. For one hyperfine component the result is plotted in Figure 2.

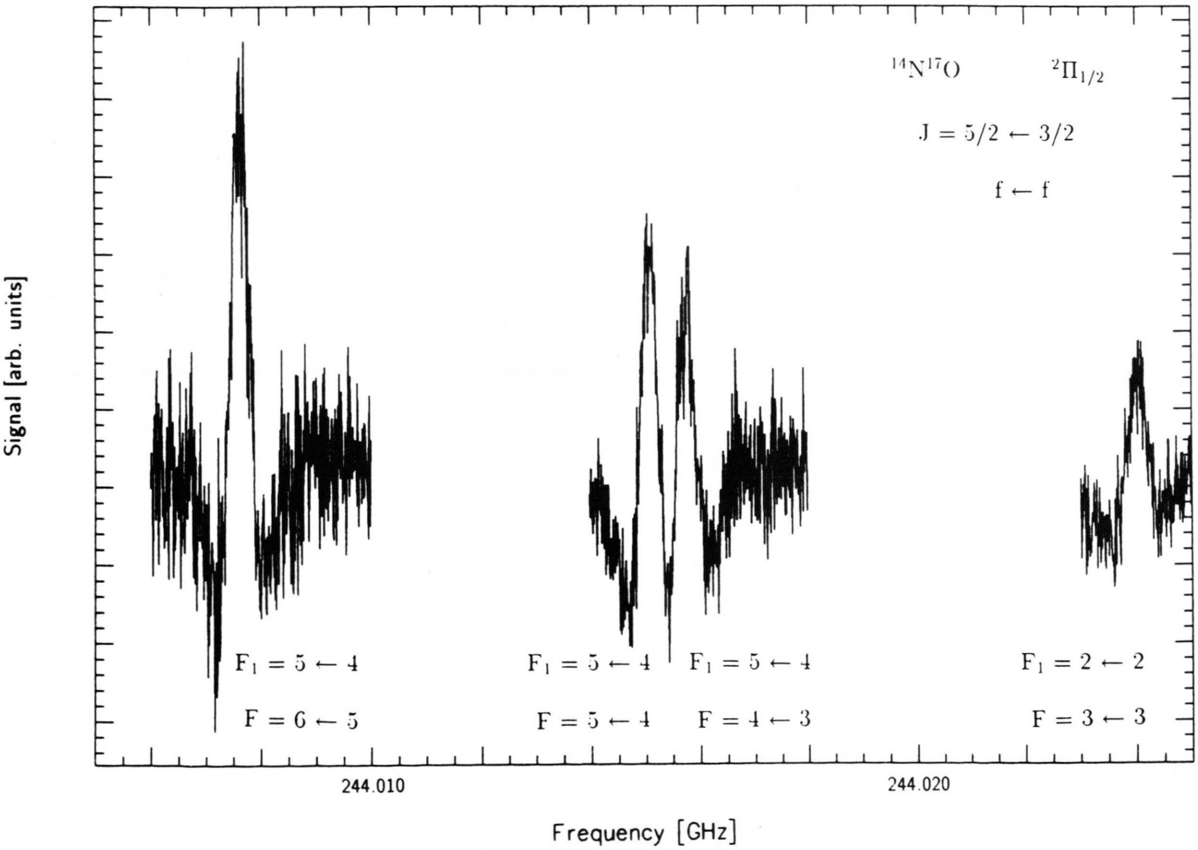

Fig. 1. $^{14}N^{17}O$: Portion of the observed hyperfine pattern at 244 GHz.

Table 1. $^{14}N^{17}O$: Observed transitions/MHz in the $X\,^2\Pi_{1/2}$ ground state.

J'	F_1'	F'	e'/f'^{*} ←	J''	F_1''	F''	e''/f''	ν_{exp}	$\Delta\nu_{exp}$[a]	exp.-calc.[b]
1.5	3	2	f	0.5	2	1	f	145 905.981	0.050	0.011
1.5	1	1	e	0.5	2	2	e	145 980.326	0.050	−0.030
1.5	3	3	f	0.5	2	2	f	145 980.326	0.050	−0.014
1.5	1	2	e	0.5	2	3	e	145 992.796	0.050	−0.019
1.5	2	3	e	0.5	2	3	e	146 041.826	0.050	0.038
1.5	2	2	e	0.5	2	3	e	146 060.465	0.050	−0.017
1.5	2	1	e	0.5	2	1	e	146 068.349	0.050	0.007
1.5	3	4	e	0.5	3	4	e	146 090.226	0.050	−0.016
1.5	3	3	e	0.5	3	3	e	146 105.562	0.050	−0.002
1.5	3	4	f	0.5	2	3	f	146 108.054	0.050	0.021
1.5	3	2	e	0.5	3	2	e	146 115.287	0.050	−0.005
1.5	3	4	e	0.5	2	3	e	146 120.882	0.050	−0.011
1.5	3	3	e	0.5	2	2	e	146 153.148	0.050	−0.006
1.5	3	2	e	0.5	2	1	e	146 171.376	0.050	−0.010
1.5	4	5	e	0.5	3	4	e	146 199.310	0.050	0.008
1.5	2	2	f	0.5	2	2	f	146 221.454	0.200	−0.059
1.5	4	4	e	0.5	3	3	e	146 222.257	0.050	−0.031
1.5	4	3	e	0.5	3	2	e	146 242.940	0.050	0.023
1.5	2	3	f	0.5	2	3	f	146 327.260	0.050	0.010
1.5	1	2	f	0.5	2	2	f	146 400.111	0.050	−0.037
1.5	4	4	f	0.5	3	4	f	146 404.473	0.050	0.030
1.5	1	1	f	0.5	2	1	f	146 410.051	0.050	0.003
1.5	1	0	f	0.5	2	1	f	146 431.036	0.050	0.016
1.5	4	3	f	0.5	3	3	f	146 446.539	0.050	−0.003
1.5	1	1	f	0.5	2	2	f	146 447.620	0.050	0.010
1.5	1	2	f	0.5	2	3	f	146 463.120	0.050	−0.027
1.5	4	5	f	0.5	3	4	f	146 490.668	0.050	0.005
1.5	4	4	f	0.5	3	3	f	146 509.095	0.050	−0.006
1.5	4	3	f	0.5	3	2	f	146 509.640	0.050	0.042
1.5	3	4	f	0.5	3	4	f	146 792.395	0.050	0.003
1.5	3	3	f	0.5	3	3	f	146 832.369	0.050	0.012
1.5	3	2	f	0.5	3	2	f	146 858.611	0.050	0.005
1.5	2	3	f	0.5	3	4	f	147 011.627	0.050	0.018
1.5	2	2	f	0.5	3	3	f	147 073.505	0.050	−0.025
2.5	4	5	e	1.5	4	5	e	243 572.996	0.030	0.017
2.5	4	3	e	1.5	4	3	e	243 578.570	0.030	−0.015
2.5	3	4	e	1.5	3	4	e	243 591.568	0.030	−0.001
2.5	0	1	e	1.5	1	1	e	243 598.128	0.030	0.017
2.5	3	3	e	1.5	3	3	e	243 599.702	0.030	−0.001
2.5	2	3	e	1.5	2	3	e	243 603.094	0.030	0.013
2.5	1	2	e	1.5	1	2	e	243 606.238	0.030	−0.013
2.5	3	2	e	1.5	3	2	e	243 606.689	0.100	−0.015
2.5	3	4	e	1.5	2	3	e	243 670.723	0.100	0.048
2.5	4	5	e	1.5	3	4	e	243 682.049	0.030	0.010
2.5	5	6	e	1.5	4	5	e	243 686.829	0.030	−0.019
2.5	4	4	e	1.5	3	3	e	243 692.988	0.030	−0.005
2.5	5	5	e	1.5	4	4	e	243 694.062	0.030	−0.013
2.5	5	4	e	1.5	4	3	e	243 702.502	0.030	0.016
2.5	4	3	e	1.5	3	2	e	243 706.227	0.030	0.017
2.5	3	3	f	1.5	2	2	f	243 868.488	0.030	0.002
2.5	3	4	f	1.5	2	3	f	243 890.322	0.100	−0.002
2.5	4	3	f	1.5	3	2	f	243 910.628	0.030	−0.021
2.5	4	4	f	1.5	3	3	f	243 924.853	0.030	0.018
2.5	4	5	f	1.5	3	4	f	243 930.698	0.030	−0.004
2.5	1	2	f	1.5	1	2	f	243 978.634	0.030	0.005
2.5	5	6	f	1.5	4	5	f	244 007.613	0.030	−0.010
2.5	5	5	f	1.5	4	4	f	244 015.071	0.030	−0.030
2.5	5	4	f	1.5	4	3	f	244 015.740	0.030	0.013
2.5	2	3	f	1.5	2	3	f	244 024.031	0.030	0.005
2.5	3	3	f	1.5	3	3	f	244 109.576	0.200	−0.083
2.5	3	4	f	1.5	3	4	f	244 109.576	0.200	0.035

* *e*/*f* denotes the parity following the notation given in [18].

[a] Estimated experimental uncertainty.

[b] Difference between measured and calculated frequencies.

Table 2. $^{14}N^{17}O$: Observed transitions/MHz in the $X\,^2\Pi_{3/2}$ ground state.

J'	F_1'	F'	e'/f'^{*} ←	J''	F_1''	F''	e''/f''	ν_{exp}	$\Delta\nu_{exp}$[a]	exp.-calc.[b]
2.5	3	4	e	1.5	2	3	e	250 522.252	0.030	0.004
2.5	3	4	f	1.5	2	3	f	250 525.156	0.030	0.012
2.5	4	5	e	1.5	3	4	e	250 594.043	0.030	0.014
2.5	4	5	f	1.5	3	4	f	250 596.554	0.030	−0.035
2.5	2	3	f	1.5	2	3	f	250 601.242	0.030	−0.004
2.5	4	4	e	1.5	3	3	e	250 603.770	0.030	−0.022
2.5	4	3	e	1.5	3	2	e	250 604.388	0.030	−0.004
2.5	4	4	f	1.5	3	3	f	250 605.975	0.030	0.016
2.5	4	3	f	1.5	3	2	f	250 606.946	0.100	0.092
2.5	3	4	e	1.5	3	4	e	250 695.737	0.030	0.012
2.5	3	4	f	1.5	3	4	f	250 698.613	0.030	−0.009
2.5	5	6	e	1.5	4	5	e	250 704.266	0.100	0.062
2.5	5	6	f	1.5	4	5	f	250 706.310	0.100	−0.005
2.5	5	5	e	1.5	4	4	e	250 724.595	0.030	0.005
2.5	5	5	f	1.5	4	4	f	250 726.350	0.030	0.005
2.5	5	4	e	1.5	4	3	e	250 738.194	0.100	0.016
2.5	5	4	f	1.5	4	3	f	250 740.114	0.030	−0.008

[a] Estimated experimental uncertainty.

[b] Difference between measured and calculated frequencies.

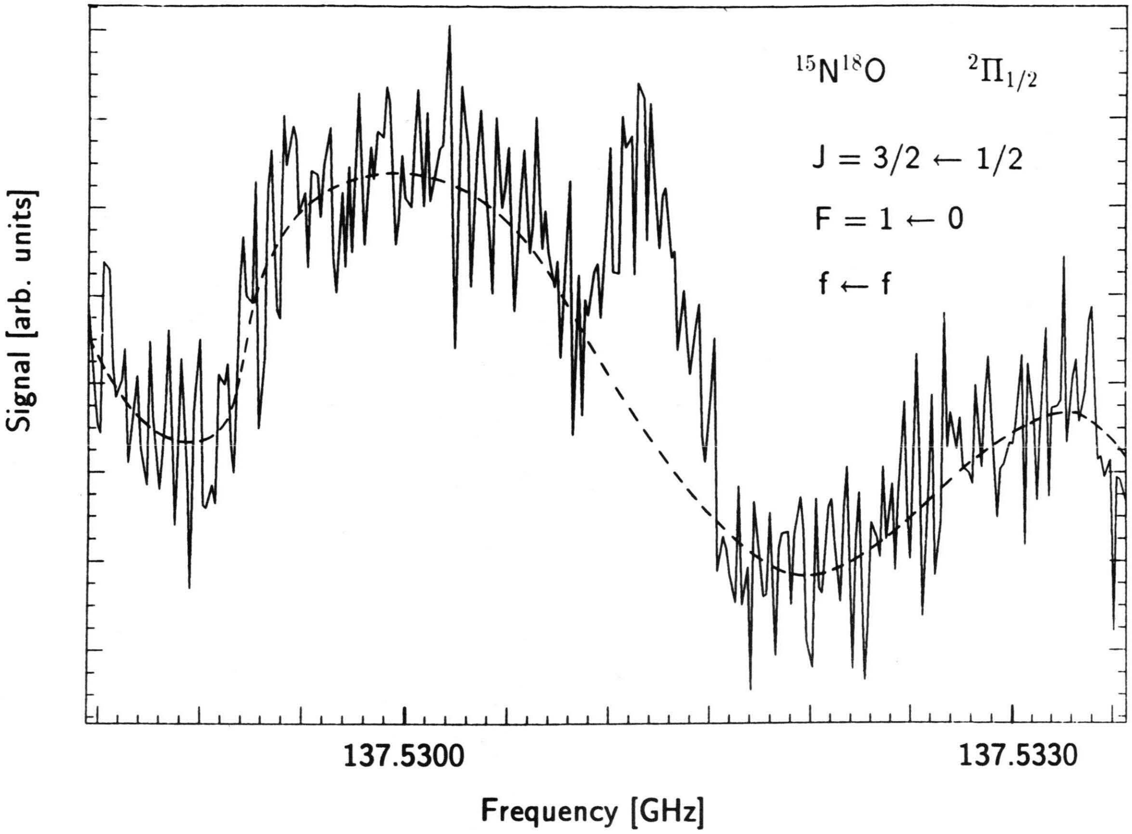

Fig. 2. $^{15}N^{18}O$: Observed hyperfine component of the lowest rotational transition at 137 GHz.

Table 3. $^{15}N^{18}O$: Observed frequencies/MHz in the $X^2\Pi_{1/2}$ and $X^2\Pi_{3/2}$ ground states.

J'	F'	$e'/f' \leftarrow$	J''	F''	e''/f''	ν_{exp}	$\Delta\nu_{exp}$[a]	exp.-calc.[b]
			$^{2}\Pi_{1/2}$					
1.5	1	e	0.5	1	e	137 241.510	0.100	−0.016
1.5	1	e	0.5	0	e	137 260.072	0.100	−0.020
1.5	2	e	0.5	1	e	137 289.744	0.100	0.003
1.5	1	f	0.5	0	f	137 531.289	0.100	0.054
1.5	2	f	0.5	1	f	137 602.977	0.100	−0.020
2.5	2	e	1.5	1	e	228 898.336	0.050	0.008
2.5	3	e	1.5	2	e	228 906.747	0.050	0.000
2.5	2	f	1.5	1	f	229 210.140	0.050	−0.007
2.5	3	f	1.5	2	f	299 224.723	0.050	−0.002
			$^{2}\Pi_{3/2}$					
2.5	2	e	1.5	1	e	235 039.429	0.050	0.013
2.5	2	f	1.5	1	f	235 041.489	0.050	−0.003
2.5	3	e	1.5	2	e	235 070.700	0.050	−0.008
2.5	3	f	1.5	2	f	235 072.651	0.050	−0.003

[a] Estimated experimental uncertainty.
[b] Difference between measured and calculated frequencies.

3. Measurements and Analysis

The matrix elements of the Hamiltonian used here for $^{15}N^{18}O$ have been published [4]. However, $^{14}N^{17}O$, bearing two non-zero nuclear spins, requires some modifications, which are given in the Appendix.

Concerning $^{15}N^{18}O$, the measurements were straightforward, based on initial frequency predictions made with the following assumed values: (*i*) Spin-orbit constants A_{eff} and A_D given in [8], (*ii*) rotational and Λ-doubling parameters of $^{14}N^{16}O$ from [4] but modified according to their reduced-mass dependence, and (*iii*) hyperfine constants of $^{15}N^{16}O$ from [4]. The observed transitions have been fitted in a least-squares procedure to determine the molecular parameters given in Table 4.

Measurement of the $^{14}N^{17}O$ species required a more thorough preparation due to the unknown ^{17}O

Table 4. $^{15}N^{18}O$: Molecular ground state parameters/MHz derived in the present study.

Parameter	This work	[8]	[4]
A_{eff}	3 691 761.8^{a}	3 691 761.8 (189)^{b}	
A_{D}	4.585 (2)^{c}	4.548 (80)	
B_{eff}	46 414.094 (6)	49 414.30 (20)	46 414.10 (12)^{d,e}
D	0.1362 (5)	0.136788 (155)	0.13663 (2)^{d}
p	319.97 (4)	319.22 (42)	319.754 (1)^{d}
q	2.24 (3)	2.323 (48)	2.3636 (1)^{d}
a	−118.143^{f}		
b	−59.024^{f}		
c	82.725^{f}		
d	−157.9474^{f}		
C_I	−0.01622^{f}		
C_I'	−0.0055^{f}		

[a] Fixed to the value from [8].
[b] Values in brackets: $1\,\sigma$.
[c] γ kept fixed to zero.
[d] Calculated from [4] using isotopic and vibrational dependences.
[e] Correction to the Born-Oppenheimer approximation applied.
[f] Value for $^{15}N^{16}O$ from [4].

Table 5. $^{14}N^{17}O$: Molecular ground state parameters/MHz derived in the present study.

Parameter	Nucleus	This work	[9]	[4]
A_{eff}		3 691 664^{a}	3 691 664	
A_{D}		5.2004 (18)^{b,c}	4.89 (54)	
B_{eff}		49 449.3908 (26)	49 449.63 (90)	49 449.40 (13)^{d,e}
D		0.15442 (23)	0.1559 (39)	0.15525 (2)^{d}
p		340.77 (4)	323 (12)	340.716 (1)^{d}
q		2.657 (24)	2.695 (22)	2.6831 (1)^{d}
a	^{17}O	−173.082 (9)		
b	^{17}O	−66.83 (17)		
c	^{17}O	93.36 (18)		
d	^{17}O	−206.122 (6)		
d_{D}	^{17}O	−0.0035 (21)		
C_I	^{17}O	−0.0281 (25)		
C_I'	^{17}O	0.010 (7)		
eQq_1	^{17}O	−1.30 (4)		
eQq_2	^{17}O	−31.5 (12)		
a	^{14}N	84.250 (24)		84.2155 (5)^{f}
b	^{14}N	41.74 (28)		42.099 (3)^{f}
c	^{14}N	−58.55 (29)		−58.989 (3)^{f}
d	^{14}N	112.591 (14)		112.5972 (1)^{f}
d_{D}	^{14}N	0.00016^{f}		0.00016 (2)^{f}
C_I	^{14}N	0.017 (4)		0.01242 (4)^{f}
C_I'	^{14}N	0.0039^{f}		0.0039 (2)^{f}
eQq_1	^{14}N	−1.83 (3)		−1.8581 (3)^{f}
eQq_2	^{14}N	21.2 (10)		23.153 (8)^{f}

[a] Fixed to the value from [9].
[b] Values in brackets: $1\,\sigma$.
[c] γ kept fixed to zero.
[d] Calculated from [4] using isotopic and vibrational dependences.
[e] Correction to the Born-Oppenheimer approximation applied.
[f] Value for $^{14}N^{16}O$.

hyperfine structure, expected to cause larger splittings than its ^{14}N counterpart. We predicted the magnetic hyperfine splitting by taking the b and c constants from the $O^{17}O$ data published by Cazzoli et al. [12], and by scaling the nuclear spin-orbit coupling constant a to the corresponding ^{14}N ratio, $\left(\frac{a}{b+c}\right)^{^{17}O} = \left(\frac{a}{b+c}\right)^{^{14}N}$. An equal procedure was applied to obtain the hyperfine Λ-doubling constant d.

The initial choice for the nuclear electric quadrupole coupling constant $eQq_1(^{17}O)$ is not essential, since the hyperfine splitting is dominated by magnetic contributions. A_{eff} and A_{D} have been taken from [9], while the rotational and Λ-doubling parameters were treated as for $^{15}N^{18}O$.

The observed doublet transitions of $^{14}N^{17}O$ at 146 509 MHZ deviated by about 10 MHz from the first prediction. Their tentative assignment led gradually to the detection and assignment of 79 transitions, resulting in the constants given in Table 5. Nine ^{17}O hyperfine structure parameters, namely a, b, c, d, d_{D}, C_I, C_I', eQq_1 and eQq_2, were determined. From the corresponding ^{14}N values, d_{D} and C_I have been taken from [4] and kept fixed. An attempt to fit a nuclear spin-spin interaction parameter did not result in a significant value; this is no surprise since the parameter is calculated to be of the order of 1 kHz.

For both isotopomers, the effective spin-orbit coupling constants A_{eff} are not well determined by the present mm-wave spectra and have been fixed to the values obtained from infrared spectroscopy. The spin-rotation constant γ cannot be determined independently from A_{D} and has subsequently been set to zero.

4. Discussion

In Tables 4 and 5, the rotational and Λ-doubling constants for $^{15}N^{18}O$ and $^{14}N^{17}O$ can be compared with the corresponding values calculated from the isotopic dependence published in [4]; the clear coincidence in B_0 confirms the values of the Born-Oppenheimer correction parameters given there. The deviation from the Born-Oppenheimer approximation is displayed in Fig. 3, where the dependence of the

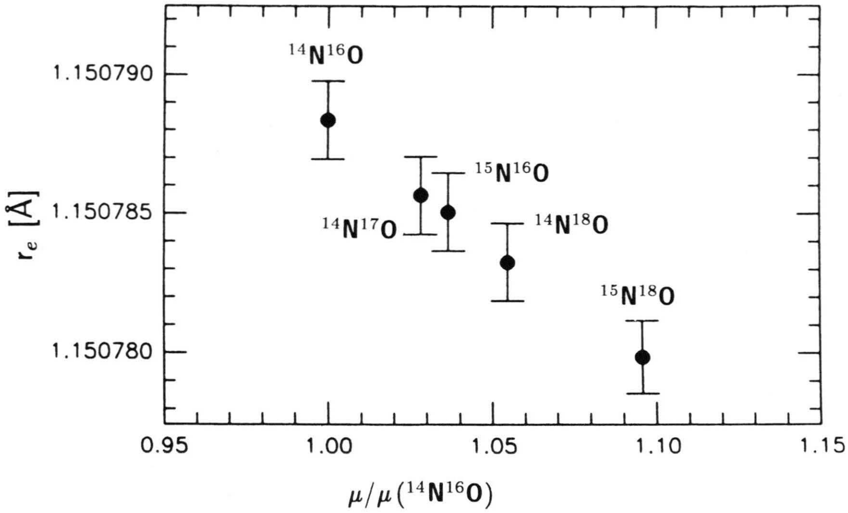

Fig. 3. No: Dependence of the equilibrium internuclear distance on the isotopic constitution. Strict validity of the Born-Oppenheimer approximation would cause the data points to lie on a horizontal line.

equilibrium internuclear distance on the isotopic constitution is shown.

In the absence of rotation-vibration interaction, hyperfine structure (hfs) is the smallest splitting that molecular spectra exhibit. Nevertheless, hfs bears information on the spatial distribution of electrons near the nuclei. In particular, the nuclear quadrupole coupling constants depend on the field gradients produced by the electrons at the nucleus. For closed-shell molecules with nuclear spin $I \geq 1$, the electric quadrupole coupling in general forms the dominant contribution to the hfs. It is accompanied by a very small shift due to magnetic nuclear-spin rotation interaction. In open-shell molecules such as NO, an additional, however more dominant hfs contribution arises from the magnetic interaction of the nuclear spin with the unpaired electron spin and the orbital angular momentum thus depending on the orbital distribution of the unpaired electron near the nucleus.

Hfs constants provide definite tests of electronic wavefunctions if the nuclear moments are known. Concerning the ^{14}N and ^{17}O nuclei, Gerber and Huber [13] and Eggenberger et al. [14] have shown that the quadrupole coupling constants eQq for several closed-shell molecules calculated by theoretical methods are in good agreement with experimentally obtained values, allowing a determination of nuclear quadrupole moments.

From the present measurement for the $^{14}N^{17}O$ molecule, a complete set of magnetic and quadrupole hyperfine coupling constants for both nuclei has been determined. These parameters enable us to derive orbital and spin distribution properties of the electrons near both nuclei, and they may also form a test of quantum-chemical calculations. It can be seen from Table 6 that orbital and spin distributions of the unpaired electron are quite similar near both nuclei (following [15], values marked by l and s derived from orbital – nuclear spin and spin – nuclear spin interaction), while the electric field gradients produced by all electrons turn out to be different for the two nuclei.

We will now turn to a brief discussion of the nuclear-spin rotation constants C_I. Townes and Schawlow [16] explained this interaction to arise mainly from the interaction with excited vibrational states (except for the case of H_2). In this framework, the ratio

$$\tilde{C}_I = \frac{C_I I}{B \mu_I/\mu_N} \propto \langle r^{-3} \rangle \sum_n \frac{|\langle \Sigma | L_x/r^3 | \Pi \rangle|^2}{E_n - E_0} \tag{2}$$

Table 6. $^{14}N^{17}O$: Spatial distribution of the unpaired electron and values for the electric field gradient near both nuclei.

Parameter	^{14}N	^{17}O	Unit
$\langle 1/r^3 \rangle_l$	14.7415 (42)	16.1419 (8)	10^{30} m^{-3}
$\langle 1/r^3 \rangle_s$	16.286 (17)	16.321 (6)	10^{30} m^{-3}
$\psi^2(0)_s$	0.464 (6)	0.398 (2)	10^{30} m^{-3}
$\langle \sin^2(\theta)/r^3 \rangle$	13.1336 (16)	12.8155 (4)	10^{30} m^{-3}
$\langle (3\cos^2(\theta)-1)/r^3 \rangle_s$	−6.830 (34)	−5.805 (11)	10^{30} m^{-3}
μ_I/μ_N [a]	0.403 760 7	−1.893 80	
$\langle \Lambda = \pm 1 \| T_0^2(\nabla E) \| \Lambda = \pm 1 \rangle$	−0.897 (15)	0.492 (15)	MHz fm^{-2}
$\langle \Lambda = \pm 1 \| T_{\pm 2}^2(\nabla E) \| \Lambda = \pm 1 \rangle$	2.12 (10)	2.44 (9)	MHz fm^{-2}
Q [b]	2.04	−2.64	fm^2

[a] from [19]; [b] from [14].

Table 7. Nuclear electric quadrupole and magnetic nuclear-spin-rotation constants in linear molecules with ^{17}O or ^{14}N nuclei.

Molecule	Nucleus	eQq_1 / MHz	C_I / kHz	$\tilde{C}_I \cdot 10^7$	Ref.
OCS	^{17}O	−1.333 (22)	−3.3 (13)	7.40 (299)	[20]
CO	^{17}O	−4.377 (56)	−30.4 (12)	7.14 (28)	[21]
$O^{17}O$	^{17}O	−8.3 (3)			[12]
OH	^{17}O	−1.92			[15]
$^{14}N^{17}O$	^{17}O	−1.30 (4)	−28.1 (25)	7.50 (67)	here
$^{14}N^{16}O$	^{14}N	−1.8581 (3)	12.42 (4)	6.05 (2)	[4]
CN	^{14}N	−1.370[a] (29)			[3]
HCN	^{14}N	−4.7091 (13)	10.4 (3)	5.81 (17)	[22]
DCN	^{14}N	−4.703 (12)	8.4 (3)	5.74 (21)	[22]
HC_3N	^{14}N	−4.3187 (29)	0.94 (39)	5.12 (212)	[17]
ClCN	^{14}N	−3.62277 (90)	1.32 (18)	5.48 (75)	[23]
ICN	^{14}N	−4.0816 (15)	0.68 (12)	5.22 (92)	[24]
C*NCN	^{14}N	−1.32152 (45)	0.82 (10)	3.93 (48)	[25]
CNC*N	^{14}N	−3.78113 (32)	0.92 (7)	4.40 (34)	[25]

[a] Converted from isotopically invariant parameters.

is proportional to this sum over excited electronic states (Π states, if the ground state is Σ or *vice versa*). Table 7 shows a compilation of eQq, C_I and $\tilde{C}_I$ values for linear molecules bearing ^{14}N or ^{17}O nuclei. According to [16], it can be expected that the mentioned ratio is approximately constant for chemically similar molecules. For the ^{14}N nucleus, Creswell et al. [17] confirmed this behaviour by comparing HC_3N with HCN. However, from an inspection of Table 7, it is found that the $\tilde{C}_I$ value for a given nucleus seems to be even roughly constant in different chemical environments, recognizable when comparing the $N={}^{17}O$ to a $C={}^{17}O$, or the $^{14}N=O$ to a $^{14}N\equiv C-$ bond. The case of CNCN, with two ^{14}N nuclei in different bonds, is fairly instructive. While the $\tilde{C}_I$ values for both nuclei agree within the uncertainties, the parameter eQq varies strongly with the chemical environment. Since the quadrupole coupling constants depend not only on the average distance of the electrons from the nucleus but also on their angular distribution, we may conclude from the presently available C_I data that for nitrogen and oxygen atoms it is essentially the angular distribution of the valence *p* orbitals that is changed in different chemical bonds, while the average radial distribution remains essentially unchanged. This behaviour is also expected to be true for other atoms of the second period, while for the third period hybridisation effects may become important. To study this aspect in somewhat more detail, more data on spin-rotation coupling constants of e.g. ^{33}S containing molecules would be desirable.

Acknowledgements

The authors would like to thank Dr. I. Pak, Troitzk, Russia, and the Research Institute for Stable Isotopes, Tbilisi, Georgia, for supplying the enriched H_2O sample. This work was supported in part by the Deutsche Forschungsgemeinschaft via Grant SFB-301.

Appendix

To deal with the more complex hfs in $^{14}N^{17}O$ due to the presence of two hyperfine interacting nuclei, the Hamiltonian matrix elements from [4] have to be modified as follows, adopting the coupling scheme $F_1 = J + I_1$, $F = F_1 + I_2$:

First, replace F by F_1 and I by I_1; mark all hyperfine constants by (1) and multiply each term by $\delta_{F_1' F_1}$.

Second, incorporate the additional matrix elements

$$\begin{aligned}
&\langle I, {}^2\Pi_{1/2}\, J';\, F_1' I;\, F \pm | H | I, {}^2\Pi_{1/2}\, J;\, F_1 I;\, F \pm \rangle \\
&\quad = + G^*(I_1, J', J, F_1', F_1, I_2, F) \left\{ (-1)^{J'-\frac{1}{2}} \begin{pmatrix} J' & 1 & J \\ -\frac{1}{2} & 0 & \frac{1}{2} \end{pmatrix} \left[a^{(2)} - \frac{b^{(2)} + c^{(2)}}{2} \right] \right. \\
&\quad\quad \left. \mp \begin{pmatrix} J' & 1 & J \\ \frac{1}{2} & -1 & \frac{1}{2} \end{pmatrix} \frac{[d^{(2)} + \delta_{J',J}\, X\, d_{\mathrm{D}}^{(2)}]}{\sqrt{2}} + 2\delta_{J'J} (-1)^{J'-\frac{1}{2}} \begin{pmatrix} J' & 1 & J \\ -\frac{1}{2} & 0 & \frac{1}{2} \end{pmatrix} X\, C_I^{(2)} \right\} \\
&\quad\quad + Q^*(I_1, J', J, F_1', F_1, I_2, F) (-1)^{J'-\frac{1}{2}} \begin{pmatrix} J' & 2 & J \\ -\frac{1}{2} & 0 & \frac{1}{2} \end{pmatrix} \frac{eQq_1^{(2)}}{4}
\end{aligned} \tag{3}$$

$$\begin{aligned}
&\langle I,\, {}^2\Pi_{3/2}\, J';\, F_1' I;\, F \pm |H|\, I,\, {}^2\Pi_{3/2}\, J;\, F_1 I;\, F \pm \rangle \\
&\quad = +G^*(I_1, J', J, F_1', F_1, I_2, F)\,(-1)^{J'-\frac{3}{2}} \begin{pmatrix} J' & 1 & J \\ -\frac{3}{2} & 0 & \frac{3}{2} \end{pmatrix} \left[a^{(2)} + \frac{b^{(2)} + c^{(2)}}{2} + \delta_{J,J'} \frac{2}{3} X C_I^{(2)} \right] \\
&\qquad + Q^*(I_1, J', J, F_1', F_1, I_2, F)\,(-1)^{J'-\frac{3}{2}} \begin{pmatrix} J' & 2 & J \\ -\frac{3}{2} & 0 & \frac{3}{2} \end{pmatrix} \frac{e Q q_1^{(2)}}{4}
\end{aligned} \tag{4}$$

$$\begin{aligned}
&\langle I,\, {}^2\Pi_{3/2}\, J';\, F_1' I;\, F \pm |H|\, I,\, {}^2\Pi_{1/2}\, J;\, F_1 I;\, F \pm \rangle \\
&\quad = -G^*(I_1, J', J, F_1', F_1, I_2, F)\,(-1)^{J'-\frac{3}{2}} \begin{pmatrix} J' & 1 & J \\ -\frac{3}{2} & 1 & \frac{1}{2} \end{pmatrix} \frac{[b^{(2)} \mp \delta_{J',J} (-1)^{J-\frac{1}{2}} (J + \frac{1}{2})\, C_I'^{(2)}]}{\sqrt{2}} \\
&\qquad \mp Q^*(I_1, J', J, F_1', F_1, I_2, F) \begin{pmatrix} J' & 2 & J \\ \frac{3}{2} & -2 & \frac{1}{2} \end{pmatrix} \frac{e Q q_2^{(2)}}{4\sqrt{6}}
\end{aligned} \tag{5}$$

with

$$\begin{aligned}
G^*(I_1, J', J, F_1', F_1, I_2, F) &= (-1)^{I_2 + 2F_1' + F + I_1 + J + 1} \begin{Bmatrix} F & F_1' & I_2 \\ 1 & I_2 & F_1 \end{Bmatrix} \begin{Bmatrix} J' & F_1' & I_1 \\ F_1 & J & 1 \end{Bmatrix} \\
&\quad \times \sqrt{I_2 (I_2 + 1)(2I_2 + 1)(2J' + 1)(2J + 1)(2F_1' + 1)(2F_1 + 1)} \\
Q^*(I_1, J', J, F_1', F_1, I_2, F) &= (-1)^{I_2 + 2F_1' + F + I_1 + J + 2} \begin{Bmatrix} F & F_1' & I_2 \\ 2 & I_2 & F_1 \end{Bmatrix} \begin{Bmatrix} J' & F_1' & I_1 \\ F_1 & J & 2 \end{Bmatrix} \\
&\quad \times \sqrt{\frac{(I_2 + 1)(2I_2 + 1)(2I_2 + 3)}{I_2 (2I_2 - 1)} (2J' + 1)(2J + 1)(2F_1' + 1)(2F_1 + 1)}\,.
\end{aligned}$$

Please note that I_1 is the nuclear spin causing major hyperfine interaction, thus in the case of $^{14}N^{17}O$: $I_1 = I^{^{17}O}$ and $I_2 = I^{^{14}N}$.

[1] J. K. G. Watson, J. Mol. Spectrosc. **45,** 99 (1973).

[2] E. Tiemann, H. Arnst, W. U. Stieda, T. Törring, and J. Hoeft, Chem. Phys. **67,** 133 (1982).

[3] A. H. Saleck, R. Simon, and G. Winnewisser, Astrophys. J. **436** (1994).

[4] A. H. Saleck, K. M. T. Yamada, and G. Winnewisser, Mol. Phys. **72,** 1135 (1991).

[5] J. K. G. Watson, J, Mol. Spectrosc. **80,** 411 (1980).

[6] Ph. R. Bunker, J. Mol. Spectrosc. **68,** 367 (1977).

[7] H. Pickett, personal communication.

[8] J. L. Teffo, A. Henry, Ph. Cardinet, and A. Valentin, J. Mol. Spectrosc. **82,** 348 (1980).

[9] C. Amiot, R. Bacis, and G. Guelachvili, Can. J. Phys. **56,** 251 (1978).

[10] K. A. and U. R. Hofmann, Lehrbuch der Anorganischen Chemie, Braunschweig 1941.

[11] D. Mauer, G. Winnewisser, and K. M. T. Yamada, J. Mol. Spectrosc. **136,** 380 (1989).

[12] G. Cazzoli, C. Degli Esposti, P. G. Favero, and G. Severi, Nuovo Cimento **62 B,** 251 (1981).

[13] St. Gerber and H. Huber, Chem. Phys. **134,** 279 (1989).

[14] R. Eggenberger, St. Gerber, H. Huber, D. Searles, and M. Welker, J. Mol. Spectrosc. **151,** 474 (1992).

[15] K. R. Leopold, K. M. Evenson, E. R. Comben, and J. M. Brown, J. Mol. Spectrosc. **122,** 440 (1987).

[16] C. H. Townes and A. L. Schawlow, Microwave Spectroscopy, McGraw-Hill, New York 1955.

[17] R. A. Creswell, G. Winnewisser, and M. C. L. Gerry, J. Mol. Spectrosc. **65,** 420 (1977).

[18] J. M. Brown, J. T. Hougen, K.-P. Huber, J. W. C. Johns, I. Kopp, H. Lefebvre-Brion, A. J. Merer, D. A. Ramsay, J. Rostas, and R. N. Zare, J. Mol. Spectrosc. **55,** 500 (1975).

[19] International Union of Pure and Applied Chemistry, Quantities, Units and Symbols in Physical Chemistry, Oxford 1988.

[20] I. Merke and H. Dreizler, Z. Naturforsch. **42a,** 1043 (1987).

[21] M. A. Frerking and W. D. Langer, J. Chem. Phys. **74,** 6990 (1981).

[22] F. de Lucia and W. Gordy, Phys. Rev. A **187,** 58 (1969).

[23] J. M. L. J. Reinartz, W. L. Meerts, and A. Dymanus, Chem. Phys. **45,** 387 (1980).

[24] J. Gripp, H. Dreizler, J. Gadhi, G. Wlodarczak, J. Legrand, J. Burie, and J. Demaison, J. Mol. Spectrosc. **129,** 381 (1988).

[25] M. C. L. Gerry, F. Stroh, and M. Winnewisser, J. Mol. Spectrosc. **140,** 147 (1990).